The stellar kinematics of galactic disks

Bottema, R

Published in:
Astronomy & astrophysics

Publication date:
1993

Astron. Astrophys. 275, 16–36 (1993)

ASTRONOMY AND ASTROPHYSICS

The stellar kinematics of galactic disks

R. Bottema

Kapteyn Astronomical Institute, University of Groningen, P.O. Box 800, NL-9700 AV Groningen, The Netherlands

Received February 26, 1992; accepted February 2, 1993

Abstract. Stellar velocity dispersion measurements of a sample of 12 galactic disks are summarized. The observed radial functionality is parameterized such that one dispersion value is assigned to each galaxy. Comparison of the galaxy dispersion with absolute magnitude and maximum rotation reveals that the dispersion is larger for the more massive systems; the relation between dispersion and intrinsic brightness of the old disk population appears to be linear. Combination of the data for face-on and inclined systems makes the conclusion plausible that the ratio between vertical and radial dispersion in external systems equals 0.6, as for the solar neighbourhood.

From the vertical disk dispersion the maximum rotation of a disk can be calculated once the ratio of scalelength to scaleheight (h/z_0) is known. This ratio is derived as a function of disk brightness from the observed dispersion for a simple one colour, one mass-to-light ratio disk model. It appears to be rather constant, possibly increasing towards the fainter systems. Then, for realistic h/z_0 values, the stellar velocity dispersions only allow the disk to have a maximum rotation of on average 63% of the observed maximum rotation. The disk is then still dominant in the central parts of the galaxy but generally the maximum disk hypothesis predicting a maximum disk rotation of 85–90% of the observed, does not apply. Exploring the consequences for the Tully–Fisher relation, it is found that this relation for disks only must be positioned at lower rotational velocities than what is observed. A dark halo and bulge must supply the additional rotation.

A relation is calculated between Toomre's Q parameter and the mass-to-light ratio for a disk. When this relation is projected onto the observed velocity dispersion – maximum rotational velocity data it is found that the same M/L ratio for galactic disks implies that the Q value is also equal for all disks, and vice versa. A universal Q value can indeed be expected when a process of self regulation is responsible for the appearance of regular spiral structure. For an $(M/L)_B$ of two which is calculated for the one colour disk model from the observed dispersion one finds Q to range between 2 and 2.5. The latter coincides with the general stability criterion for galaxies as derived in numerical experiments.

Finally, the effect of a dark halo on the observable velocity dispersion has been investigated. It appears that the hitherto adopted radially decreasing dispersion proportional to the square root of the surface density, as expected for an isolated disk, is a good approximation. This is certainly valid for radii within two scalelengths for which dispersions have been measured.

Key words: general – kinematics and dynamics – structure of

1. Introduction

Observing the stellar velocity dispersion of galactic disks is difficult. At first because disks of galaxies are very faint and consequently long integration times at large telescopes are needed. Secondly the dispersions are relatively small requiring a high dispersion spectrograph setup which dilutes the available light. An additional problem is the laborious and intricate procedures which are involved when reducing and interpreting the absorption line spectroscopy. So it is no wonder that dispersion data have become available for only a few disks. The first publications are by van der Kruit & Freeman (1984, 1986), the latter of the galaxies NGC 5247 and NGC 7184, followed by a sequence of papers by Bottema et al. (1987, 1991) and Bottema (1988, 1989a, b, 1990, 1992) making up a sample of 11 disks with measured dispersion. The sample has been extended with data for our Galaxy obtained by Lewis & Freeman (1989). The most important conclusion from these works was that the velocity dispersion decreases exponentially as a function of radius, reconciling constant thickness with a constant M/L ratio. This dispersion behaviour is such that the value of Toomre's Q parameter is nearly constant throughout the disk. Other velocity dispersion observations of external systems exist, but only of the brighter bulges (Whitmore et al. 1985) and/or bars (Jarvis et al. 1988) or bar dominated galaxies (Kormendy 1983, 1984).

Knowledge of random motions is important because it provides a direct measure of the local surface density.

Comparison with results from rotation curve analyses will then give insight into the distribution and amount of dark matter associated with a galaxy. Measurements of velocity dispersions will also contribute to our understanding of disk stability. It is known that cold isolated disks cannot exist but that both a dark halo and appreciable internal stellar motions tend to stabilize a galaxy (Spitzer & Schwarzschild 1951; Toomre 1964; Ostriker & Peebles 1973). Recent numerical simulations by a.o. Efstathiou et al. (1982), Sellwood & Carlberg (1984) and Athanassoula & Sellwood (1986) give a description of the conditions a stable galaxy has to obey. It appears that the dispersion measurements, when compared with the results of these numerical calculations, give useful information about stability and evolution of a galactic disk.

In the present paper the data of all disks are combined and compared. The possible analyses noted above have been performed and important conclusions are reached especially concerning mass content, mass distribution and stability. Resulting implications for the Tully–Fisher relation are discussed. In each section separately there is a discussion of the derived results. So at the end of the paper, in Sect. 10, only a few general points are addressed and some possible future research items are proposed. In Sects. 2 and 3 the available dispersion measurements are combined, parameterized and compared. Sections 4 to 7 describe the implications of the observed dispersions. Sections 8 and 9 can be read more or less separately; being a reanalysis of previous observations and a justification of the adopted dispersion functionality. Unless stated otherwise, a Hubble constant of $75\,\mathrm{km\,s^{-1}\,Mpc^{-1}}$ has been adopted.

2. Dispersion as a function of radius

A locally isothermal galactic disk has a space density ρ

$$\rho(R,z)=\rho(R,0)\ \mathrm{sech}^2\left(\frac{z}{z_0}\right). \tag{1}$$

If the mass-to-light ratio is constant this translates into a space light density l

$$l(R,z)=l(R,0)\ \mathrm{sech}^2\left(\frac{z}{z_0}\right), \tag{2}$$

which proves to be a good description of the actually observed light distribution in edge-on galaxies, at least away from the thin dust lane. Moreover, the thickness parameter z_0 appears to be constant over the whole disk (van der Kruit & Searle 1981a, b; 1982). Such an isothermal disk obeys

$$\langle v_z^2\rangle^{1/2}=\sqrt{\pi G\sigma(R)\ z_0}, \tag{3}$$

where $\sigma(R)$ is the surface density. For a constant M/L, constant z_0 disk then

$$\langle v_z^2\rangle^{1/2}\propto\sqrt{\mu(R)} \tag{4}$$

or, the stellar velocity dispersion in the perpendicular direction is proportional to the square root of the surface brightness $\mu(R)$. Some mechanism heats up the stars (Spitzer & Schwarzschild 1951; Carlberg & Sellwood 1985) and although this mechanism is still poorly understood (Binney & Lacey 1988) it can reasonably be expected that the dispersion in the radial direction is closely coupled to that in the perpendicular direction. Then also the radial velocity dispersion should be proportional to $\sqrt{\mu(R)}$. Most disks are close to exponential. For such a disk, with scalelength h, the dispersion is proportional to $\mathrm{e}^{-R/2h}$.

The situation just sketched is for an ideal, one stellar component isolated disk. For a disk embedded in a dark halo corrections are necessary, which are generally small, certainly for the inner two scalelengths where dispersions are measured. In Sect. 9 an ample discussion of this matter is presented. One may question whether the z-distribution of disk stars is really isothermal. This has been discussed in detail by van der Kruit (1988). He concludes that near the plane a deviation from isothermal may occur but certainly an exponential distribution as proposed by Wainscoat et al. (1989) is too extreme and not in concordance with dispersion measurements of old disk stars in the solar neighbourhood. As a compromise van der Kruit proposes a sech z-distribution which is likely the distribution which constitutes the largest possible deviation from isothermal. For a sech density distribution a measured vertical velocity dispersion would lead to a 17% larger derived surface density than for the isothermal case. In this respect it is worth noticing the recent observations by Aoki et al. (1991) of the edge-on galaxy NGC 891. At least for the approaching side of the galaxy where one is looking at the front side of a spiral arm, they observe in the K-band at small heights ($z<0.5$ kpc) a thin layer well fitted by an exponential profile with a scaleheight of 350 pc. This layer is thinner than the disk thickness (scaleheight of 500 pc) measured in B and I at large heights. Aoki et al. therefore conclude that the light in K originates from a young component which mainly comprises M-supergiants resulting from recent star formation in spiral arms. Such a young component emits large amounts of near infrared light but has an insignificant mass density. This demonstrates that near infrared light enhancements near the galactic plane are most likely caused by star formation activity and are not an indication of a mass concentration at small heights exceeding the isothermal vertical profile. Presently, Eqs. (1)–(4) will be regarded to remain a good description of a stellar disk and certainly of the mass dominant old stellar population. As will be discussed below, the implications of a deviation from isothermal will not seriously influence the final conclusions.

For a number of galaxies the stellar velocity dispersion of the disk has now been determined (see references introduction). Inclined galaxies give the radial and tangential dispersions, while in close to face-on galaxies the dispersion in the z-direction dominates. In Fig. 1 for all

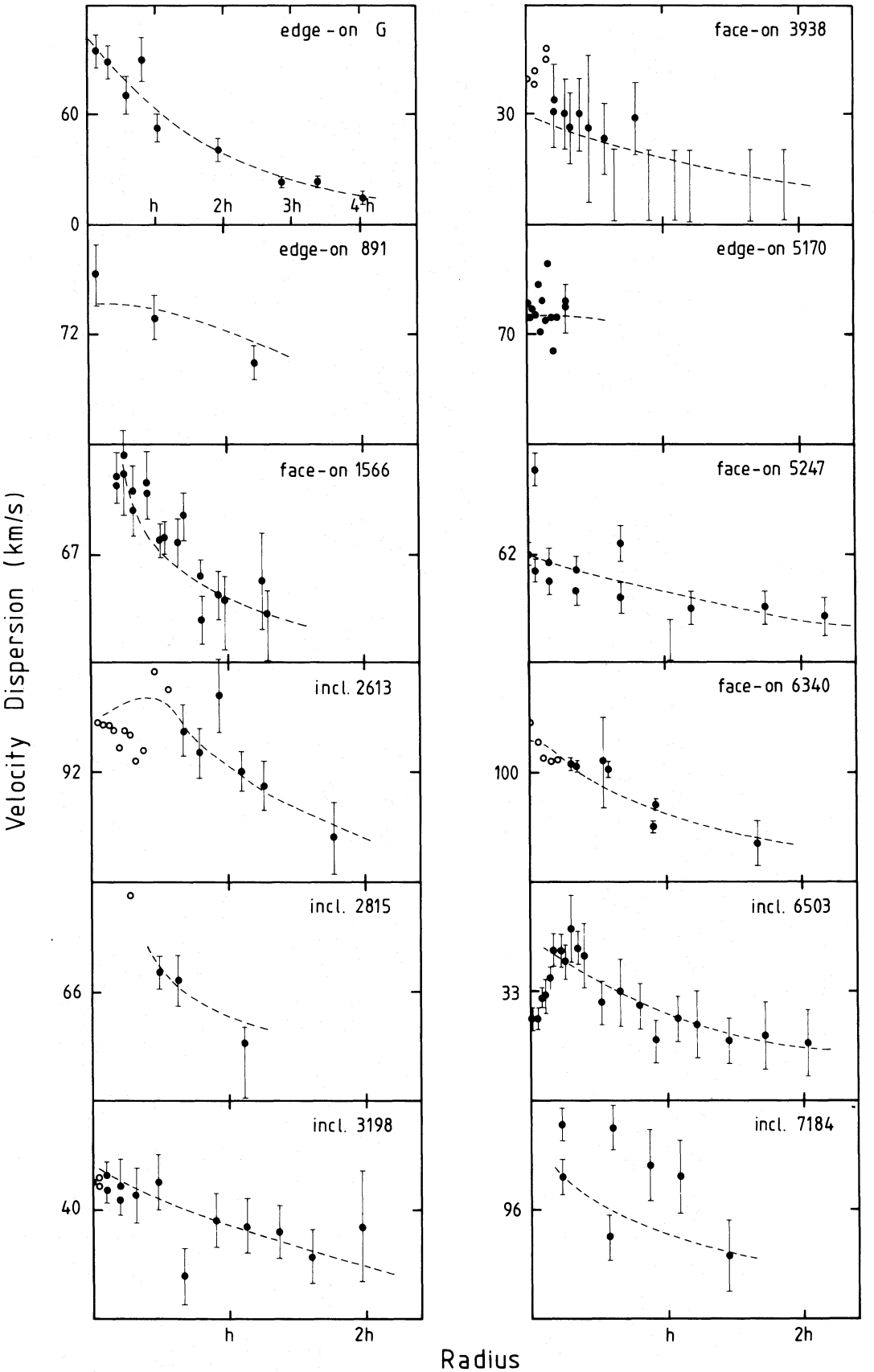

Fig. 1. Review of the observed velocity dispersion for the sample of galaxies. Data are presented as a function of distance from the position of maximum light intensity in units of optical scalelength (h). Filled circles are disk dominated, open circles bulge dominated. The dashed line indicates a fit to the data for an internal dispersion in the radial direction decreasing exponentially with a scalelength twice the photometric scalelength for the disk, and constant bulge dispersion

galaxies the radial behaviour of the dispersion is shown. Superposed are curves which indicate the predicted functionality for a dispersion proportional to $\sqrt{\mu(R)}$. These curves are obtained by taking into account line of sight integration effects and the contribution of an isothermal bulge. The results for the individual galaxies will be discussed briefly.

N 6503. Beautifully decreasing velocity dispersion proportional to $e^{-R/2h}$. Only near the centre there is a puzzling drop in the dispersion. Note that the dispersions are very small for this faint galaxy.

N 3198. A dispersion $\propto e^{-R/2h}$ fits the data nicely.

G. Data from Lewis & Freeman (1989). Their adopted scalelength is 4.4 kpc and the distance to the galactic centre 8.5 kpc.

N 891. Spectra were obtained by putting the spectrograph slit perpendicular to the major axis at three radial positions on this edge-on galaxy. Data were fitted by including a proper treatment of the absorption layer and by assuming a bulge dispersion of 110 km s^{-1}.

N 5170. This galaxy is close to edge-on ($i=86°$). Even near the centre the influence of the bulge is negligible.

N 2815. This galaxy is dominated by the bulge for $R<20''$. A constant dispersion bulge and exponential disk give a good fit to the data.

N 7184. Observations by van der Kruit & Freeman (1986) reanalysed in this paper, Sect. 9. The dispersions for this large Sc galaxy are irregular; there is a considerable difference between the two sides. The presented curve therefore is mainly the result of the dispersions determined from a fit to the observed asymmetric drift.

N 2613. Only the result for the east side is shown. The stellar velocity field for the West side is too irregular to allow a proper interpretation. Likely this galaxy has undergone a merging event in the recent past. Because of lack of photometry the scalelength is ill defined.

The face-on galaxies

N 3938. The dispersion is small. In the outer region values are below the resolution limit.

N 5247. Except for the one discrepant point the dispersion decreases regularly proportional to the square root of the surface brightness.

N 6340. The only Sa system in the sample.

N 1566. The curve is the result of the H-band photometry. There is a colour $(B-H)$ gradient giving a good result for a constant M/L H-light. In the B-band a change in M/L is needed.

A general conclusion is certainly that both the radial and perpendicular dispersion decrease with radius in a way consistent with constant M/L and thickness. For the galaxies with a better resolution like NGC 6503, 3198, 5247 and 1566 a dispersion proportional to the square root of the surface brightness fits the observations very well.

For the smaller galaxies the stellar velocity field is regular. The errors in the data are because of the limited instrumental resolution. The larger galaxies on the other hand have a larger dispersion and one is less limited by the instrument. But the stars do not seem to rotate very regularly making the interpretation less straightforward. Possibly the capture of small satellite galaxies may have distorted the velocity field.

3. Representing the disk dispersion

To compare the stellar kinematics of the individual galactic disks the dispersion has to be parameterized. It has been chosen to represent the disk dispersion of the inclined galaxies by the radial dispersion value at a radius of one (blue) scalelength. For the face-on galaxies the extrapolated value of the z-dispersion at the centre will be taken. Always, of course, for dispersion values obtained after properly taking into account integration effects and bulge contributions. The reason for this way of representing the data is that for an exponential disk $\langle v_R^2\rangle_{R=h}^{1/2}=0.6\times\langle v_R^2\rangle_{R=0}^{1/2}$ and in the solar neighbourhood $\langle v_z^2\rangle_{\odot}^{1/2}=0.6\times\langle v_R^2\rangle_{\odot}^{1/2}$. So, if the constant factor 0.6 between R and z-dispersion for the solar neighbourhood applies for all galaxies; $\langle v_R^2\rangle_{R=h}^{1/2}$ and $\langle v_z^2\rangle_{R=0}^{1/2}$ should be comparable.

For the galaxies of the sample the dispersion is related to what is essentially the mass content of the galaxy in Tables 1 and 2. The first way to describe this mass content and then especially the content of the disk is by giving the absolute luminosity of the old disk population ($M_{\rm od}^B$). This is obtained by subtracting from the total light the contribution of the bulge and of the young disk population. Then, what is left is a quantity which represents the mass of the stellar disk and is likely closely related to the disk dispersion. Absorption corrected luminosity values are taken from the Shapley-Ames catalog (Sandage & Tammann 1981) and from van der Kruit (1986) for our Galaxy. Only for NGC 891 a special procedure has been followed; from the dust model of Kylafis & Bahcall (1987) for this galaxy a total absorption of $\sim$0.92 mag can be calculated. Applying this internal absorption correction to the luminosity of Sandage & Tammann (1981) gives an absolute luminosity of ~ -20.3. A second way to represent the mass of the galaxy is by giving the maximum rotational velocity. For the inclined systems it is observed; for the close to face-on systems the Tully–Fisher maximum rotation is given determined from Rubin et al. (1985). The rotation is for the total galaxy, so for systems with an appreciable bulge like NGC 2815 and 2613 it has to be taken into account that, when compared with the disk dispersion, the rotation is somewhat too large.

Table 1. Absolute luminosities

Galaxy	Hubble type	$M_T^{Bo,i}$ total (mag)	Bulge/disk light in B	M_T^B disk (mag)	$B-V$ (mag)	(%) o.d.	M_{od}^B (mag)
N 6503	Sc	-18.76	0	-18.76	0.8	75	-18.45
N 3198	Sc	-19.51	0	-19.51	0.6	52	-18.80
G	Sb	-20.3 ± 0.2	0.14	-20.2	0.84	80	-19.97 ± 0.3
N 891	Sb	—	0.17	-20.3	Est. 0.84	80	-20.07 ± 0.3
N 5170	Sb:	-20.58	0	-20.58	Est. 0.7	63	-20.08
N 2815	Sb	-21.12	1:2	-20.76	Est. 0.84	80	-20.43
N 7184	Sb	-22.22	0	-22.22	0.7	63	-21.72
N 2613	Sb	-22.71	Est. 1:2	-22.26	Est. 0.84	80	-22.02
N 3938	Sc	-19.66	0	-19.66	0.5	42	-18.72
N 5247	Sc	-20.21	0	-20.21	0.55	47	-19.39
N 6340	Sa	-20.17	0.24	-19.94	1.0	100	-19.94
N 1566	Sc	-21.41	0	-21.41	0.8	75	-21.09

Table 2. Kinematical properties

Galaxy	h_B (arcsec)	h_B (kpc)	z_0 (pc)	v_{rot}^{max} (km s^{-1})	v_{rot}^{max} T–F (km s^{-1})	$\langle v_R^2\rangle_{R=h}^{1/2}$ (km s^{-1})	$\langle v_z^2\rangle_{R=0}^{1/2}$ (km s^{-1})
N 6503	40	1.16		120		33 ± 4	
N 3198	58	2.5		160		40 ± 7	
G	—	4.4	700	220		60 ± 10	
N 891	107	4.9	990	225		72 ± 12	
N 5170	70	6.8	970	250		70 ± 15	
N 2815	46.3	6.73		285		66 ± 12	
N 7184	48	8.4		270		96 ± 25	
N 2613	18→42	2→4		315		92 ± 32	
N 3938	36	1.75			147 ± 20		30 ± 8
N 5247	40	3.1			165 ± 20		62 ± 10
N 6340	28	2.7			270 ± 40		100 ± 20
N 1566	35.7	2.6			212 ± 30		67^{+26}_{-14}

In Figs. 2 and 3 the velocity dispersion is given as function of old disk luminosity and maximum rotational velocity respectively. There appears to be a more or less linear relation, in the sense that the more luminous, larger galaxies have a larger dispersion. In the dispersion luminosity relation only NGC 6340 has a somewhat too large dispersion which might be explained by the different Hubble type: Sa instead of Sb-c. For the maximum rotation dispersion figure, NGC 2815 has a rather large rotation for its dispersion which, as discussed above, is due to the bulge. In Fig. 2 a line has been fitted to the data by eye given by

$$\langle v_R^2\rangle_{R=h}^{1/2}=\langle v_z^2\rangle_{R=0}^{1/2}=-17\times M_{od}^B-279\ \mathrm{km\,s^{-1}}. \quad (5)$$

The dispersions of the inclined and face-on galaxies show the same functionality. Although the number of data points is still limited it can reasonably be concluded that the vertical velocity dispersion is 0.6 times the radial dispersion over the luminosity range of the observed galaxies. Certainly there is no indication that $\langle v_z^2\rangle^{1/2}/\langle v_R^2\rangle^{1/2}$ changes when the galaxy brightness changes. The factor 0.6 holds for the solar neighbourhood. It also follows from numerical experiments by Villumsen (1985), who simulated the evolution of a 3d galactic disk. Because of these three facts it will be adopted that the factor 0.6 between z and R dispersion is valid for all galactic disks.

4. The mass-to-light ratio and scale height

Two relations have been found in the previous section of which the first, dispersion versus brightness, will be analysed presently. To that aim the concept of a galaxy will be considerably simplified keeping in mind that every derived relation or result has a considerable scatter superposed on it. Of a galaxy the bulge will be ignored (Sb or Sbc) or the light of the bulge will be subtracted as in Table 1. The

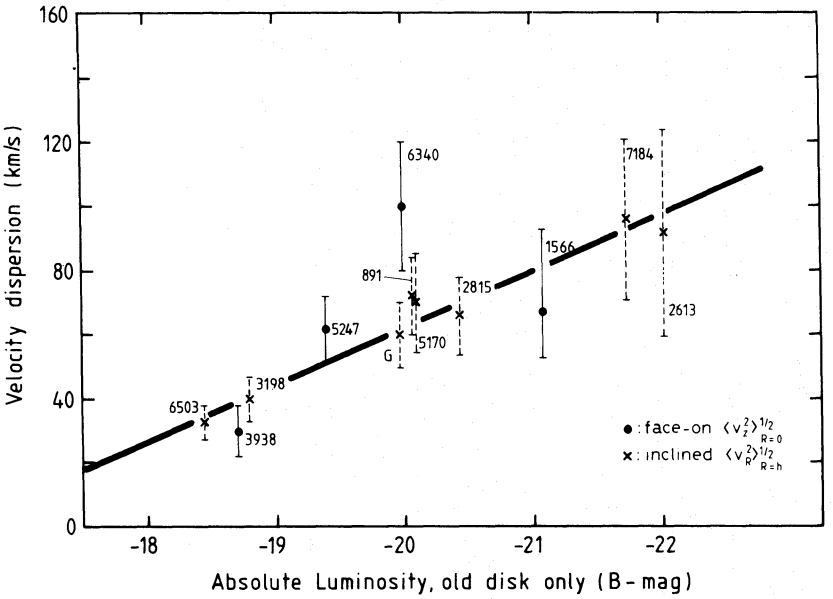

Fig. 2. Representative velocity dispersion for the different galaxies as a function of absolute luminosity of the old disk. The values are tabulated in Tables 1 and 2. By eye a linear relation [Eq. (5)] has been fitted to the data

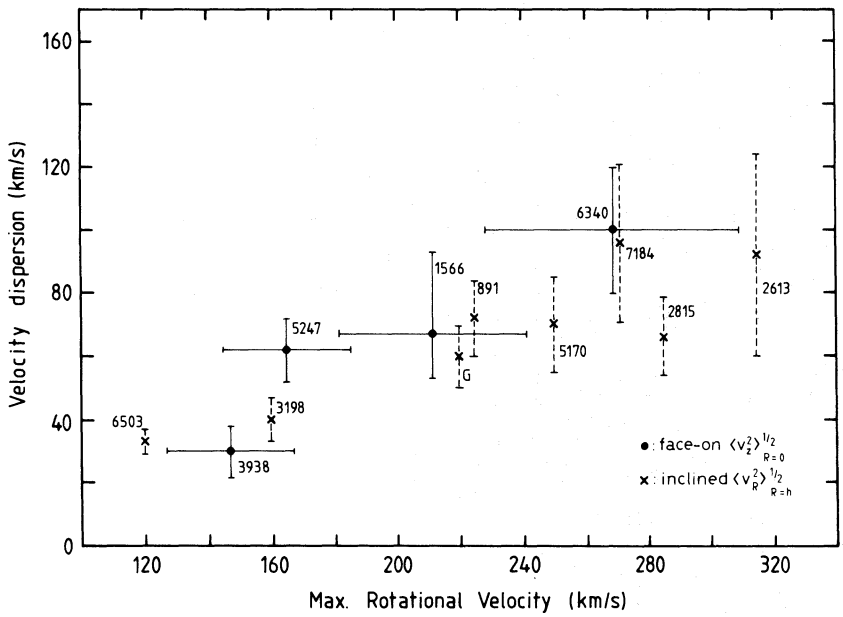

Fig. 3. Representative velocity dispersion for the sample of galaxies as a function of maximum rotational velocity. For the inclined systems this velocity is observed, for the face-on systems the Tully–Fisher value is used

resulting galactic disk is assumed to be exponential, locally isothermal and have a constant M/L ratio [Eqs. (1) and (2)]. Incorporated is the result of the previous section that $\langle v_z^2\rangle^{1/2}/\langle v_R^2\rangle^{1/2}=0.6$ for all galactic disks and that Eq. (5) holds with a certain error. Then according to Eq. (3)

$$\langle v_z^2\rangle^{1/2}_{R=0}=\sqrt{\pi G\sigma_0 z_0} \tag{6}$$

and

$$\langle v_z^2\rangle^{1/2}_{R=0}=\sqrt{\pi G\mu_0\left(\frac{M}{L}\right)z_0}, \tag{7}$$

where σ_0 and μ_0 are the extrapolated central surface density and brightness respectively. Some manipulation with Eq. (7) yields

$$\frac{M}{L}=5.27\left(\frac{\langle v_z^2\rangle^{1/2}_{R=0}}{50\ \mathrm{km\,s^{-1}}}\right)^2\left(\frac{\mu_0}{50L_\odot\ \mathrm{pc}^{-2}}\right)^{-1}\times\left(\frac{h}{z_0}\right)\left(\frac{h}{0.7\ \mathrm{kpc}}\right)^{-1}. \tag{8}$$

A relation between the mass-to-light ratio and scalelength divided by scaleheight (h/z_0) will be derived from this formula. The dispersion is given by the observations summarized in Eq. (5). For the central surface brightness the value from Freeman's law (Freeman 1970; van der

Kruit 1987a) will be used which has an 0.4 mag scatter to it. The scalelength follows from

$$L_{\rm tot}=2\pi\mu_0 h^2, \tag{9}$$

the relation between total luminosity of a galactic disk and its brightness and size. Again Freeman's law was used and h calculated. Summarized in Table 3 are the relevant values and relations for the Johnson B and Gunn & Thuan r bands. One further simplification was adopted, namely $B-V=0.7$ for all galactic disks such that

$$\text{for } B-V=0.7\text{: } M^B_{\rm gal\ disk}=M^B_{\rm od}-0.5. \tag{10}$$

Substitution into Eq. (8) gives

$$\left(\frac{M}{L}\right)_B\left(\frac{z_0}{h}\right)=1.04\left\{\frac{-17M^B_{\rm od}-279}{\rm km\ s^{-1}}\right\}^2 10^{0.2M^B_{\rm od}}. \tag{11}$$

To assess this relation the resulting h/z_0 for a constant mass- to-light ratio of for example 2.0 will be studied. The result is in Fig. 4a and shows an h/z_0 decreasing from 11 for the faint galaxies to a constant level of about 5.2 for the normal and bright galaxies. On the other hand, a constant h/z_0 of five gives a mass-to-light ratio around 2.0 over most of the brightness range (Fig. 4b). What generally can be concluded is that the observed velocity dispersions imply that a constant M/L ratio results in a rather constant h/z_0 ratio and vice versa.

Changing $B-V$ from the canonical value of 0.7 only slightly changes the scalelengths of a disk and hence also the $(M/L)_B$ ratio remains nearly equal. In the calculations above an average mass-to-light ratio is derived, where average means averaged over Hubble type or colour of a disk. This because for all disks one value of the central extrapolated surface brightness has been used, simply because a Hubble type dependence of μ^B_0 is not observed (van der Kruit 1987a; Disney & Phillipps 1985). If galactic disks are comparable, however, one would expect the later types to be brighter in the B band, because there is more star formation going on. It might be that this is not observed because later types also contain more dust, thus obscuring the extra light and making Freeman's law independent of Hubble type. Anyway, with respect to the calculations above, present information only allows to draw conclusions for one type of idealized disk. In that respect, the value of $(M/L)_B$ of about 2.0 compares well with the stellar $(M/L)_B$ values of population models by Larson & Tinsley (1987).

Several arguments can be given in favour of an equal M/L ratio for all galactic disks, where M/L is corrected for population effects or applying to the old stellar population only. Saying it differently: arguments for equal M/L ratios for all galactic disks if these disks have the same colour. I shall give some of these. First an important although "soft" argument, namely that it is common practice to take a constant M/L in a galactic disk while the brightness ranges over more than four scalelengths. For a comparable brightness range among different galaxies it should then just be the same common practice to take an equal M/L ratio for these galaxies. A second argument is given by galactic evolution models of Larson & Tinsley (1978). It appears that there is no need for different initial mass functions and hence stellar M/L ratios to explain the observed galaxy colours. A third argument is formed by a combination of the familiar Freeman's law (equal "L") and similar central surface density for all galaxies (equal "M"). The latter follows naturally from calculations of galaxy formation with detailed conservation of angular momentum (Fall & Efstathiou 1980) when the visible mass is always a constant fraction of the total mass (van der Kruit 1987a; Fall 1983). Related to the last argument is that equal mass-to-light ratios are required to make the Tully–Fisher relation apply over the observed range of galaxy luminosities. Furthermore, in Sect. 7 evidence is presented that the same Toomre's (1964) Q value for different disks implies equal M/L's. If one mass-to-light ratio can be adopted, its value can be fixed through Eq. (11) and by observing that $h/z_0=5.1\pm1.5$ for a number of galaxies of size comparable to our Galaxy (van der Kruit & Searle 1982). Then $(M/L)^B_{\rm od}\sim2.0$ and the ratio of scaleheight to scalelength goes as in Fig. 4a. To give an idea of the numbers involved, in Table 4 values for h and z_0 are given for different brightnesses. The result is very reasonable but it should be remembered that it is derived for a highly idealized galaxy. In practice there will be a scatter as can already be noticed by comparing the scalelengths with the ones given for the observed sample in Table 1. Reasons for this scatter are likely: still a small scatter in the individual M/L's, a deviation of a galactic disk from the exponential nature and a scatter in the dispersion luminosity relation caused by different heating–cooling rates for the different galaxies.

Table 3. Freeman's law

Passband	Central brightness (mag arcsec^{-2})	Scalelength (pc)
Johnson B	$\mu^B_0=21.65=136\ L_\odot\ {\rm pc}^{-2}$	$h=0.413\ 10^{-0.2M^B_{\rm gal\ disk}}$ $=0.52\ 10^{-0.2M^B_{\rm od}}$ for $B-V=0.7$
Kodak IIIa–J	$\mu^J_0=21.5=136\ L_\odot\ {\rm pc}^{-2}$	$h=0.385\ 10^{-0.2M^J_{\rm gal\ disk}}$
Gunn & Thuan r	$\mu^r_0=\ \ \ 195\ L_\odot\ {\rm pc}^{-2}$	$h=0.264\ 10^{-0.2M^r_{\rm gal\ disk}}$

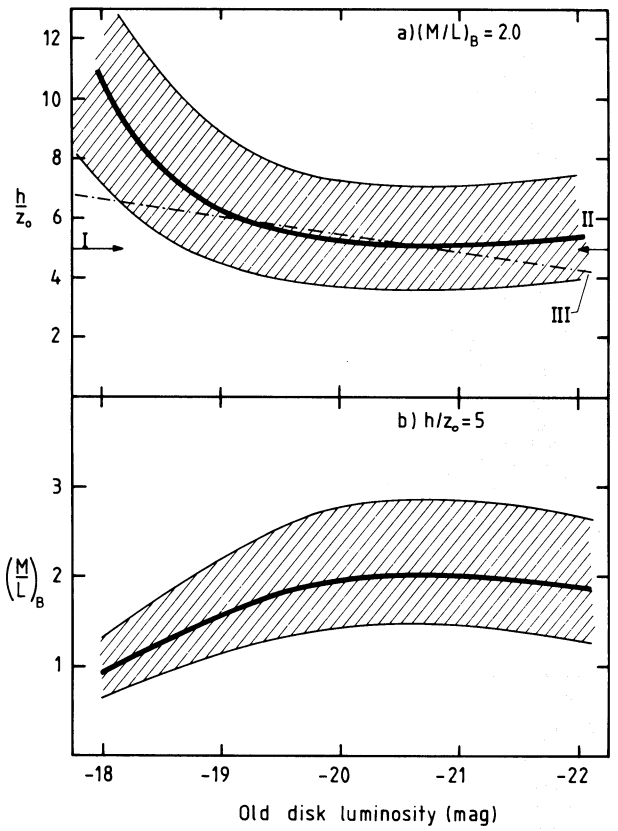

Fig. 4a and b. Predicted functionality of h/z_0 and $(M/L)_B$ as a function of galaxy absolute luminosity for the linear dispersion relation of Fig. 2. **a** Resulting h/z_0 for equal mass-to-light ratios, where the error, given by the shaded region, results from the 0.4 mag scatter of Freeman's law. Roman numbers I to III indicate model lines used in Sect. 6. **b** Resulting mass-to-light ratio for an equal h/z_0 of 5.0 for all galaxies

Table 4. Scalelength and height of a disk with $(M/L)_B = 2.0$

M^B_{od} (mag)	h (kpc)	h/z_0	z_0 (pc)
−18	2.07	10.8	191
−19	3.28	6.3	520
−20	5.20	5.2	1000
−21	8.24	5.1	1616
−22	13.06	5.2	2420

To put matters in a broader perspective the discussion will be extended to the r-band of Thuan & Gunn (1976). A rough conversion from the B to the r-band is given by $M^r_{od} \sim M^B_{od} - 1.0$ (Kent 1986). For the poor man's population synthesis used by Bottema (1988) for a galactic disk with $B-V \sim 0.7$, $M^r_{gal\ disk} \sim M^r_{od} - 0.2$ which results in

$$M^r_{gal\ disk} \sim M^B_{od} - 1.2, \qquad (12)$$

but the results of the discussion do not depend sensitively on the exact passband conversion. Equation (12) can now be substituted into Eq. (5) to obtain a dispersion luminosity relation in the r-band

$$\langle v_z^2 \rangle^{1/2}_{R=0} = -17 M^r_{gal\ disk} - 300\ \mathrm{km\,s^{-1}}, \qquad (13)$$

and the $(M/L)_r - (h/z_0)$ relation can be derived

$$\left(\frac{M}{L}\right)_r \left(\frac{z_0}{h}\right) = 1.43\ (-17 M^r_{gal\ disk} - 300)^2\ 10^{0.2 M^r_{gal\ disk}}. \qquad (14)$$

For a constant h/z_0 of five the resulting mass-to-light ratios are given in Fig. 5, and for an h/z_0 changing as in Fig. 4a, $(M/L)_r = 1.55$, constant. Superposed on these values is the scatter of 0.4 mag of Freeman's law. The relation in Fig. 5 is compared with $(M/L)_r$ values derived by Kent (1986, 1987) resulting from a maximum disk fit (van Albada & Sancisi 1986) to the rotation curve. Only Sc and Sbc galaxies are considered to avoid any bulge confusion and data have been converted to a Hubble constant of 75 $\mathrm{km\,s^{-1}\,Mpc^{-1}}$. Absolute luminosities are taken from the Shapley–Ames catalog of which from the B-band values 1.0 has been subtracted to convert to the r-band. Inspection of Fig. 5 learns that the approximate or exactly constant relation derived from the dispersions constitutes a lower boundary to the maximum disk M/L ratio's. This is in fact what is to be expected because of two reasons. First, the maximum disk ratio's can be too large because L is too small which is caused by internal absorption in the galaxy. There is evidence, although marginal, that M/L is larger for larger inclinations (Kent 1986) to be explained by this absorption.

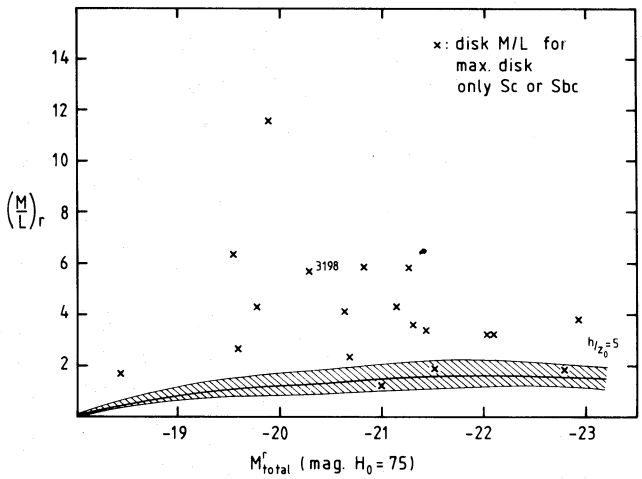

Fig. 5. Mass-to-light ratios in the r-band for different galaxy luminosities. The line indicates the values expected for a linear function fitted to the data in Fig. 2 with constant h/z_0 of five. Crosses are the values of maximum disk fits for individual galaxies of the Kent (1986, 1987) sample. Only Sc and Sbc systems are included so that the galaxies are essentially disk only systems, just for reference the data point of the galaxy NGC 3198 has been indicated. The line constitutes a lower boundary to the data, indicating that the maximum disk M/L's are larger than what one can expect on the ground of the observed velocity dispersion

But reasonable allowance is made for this by the error in Freeman's law which is determined for a number of galaxies with various inclinations. So, the shaded area in Fig. 5 should already include most of the absorption effects. The second explanation, and to my opinion the more favourable, for the higher maximum disk M/L's is that M is determined too large because maximum disk does not apply in all cases. Then in principle all mass-to-light ratios of a disk scatter around or just above (because of absorption) the value of 1.55. Higher observed maximum disk M/L's originate from the contribution of a dark halo.

5. The maximum rotation

The second relation found in Sect. 2, namely dispersion versus maximum rotational velocity will now be discussed. In Eq. (6) the dispersion is given resulting from a certain surface density. For an infinitely thin stellar disk the surface density can be related to the maximum rotational velocity (Freeman 1970) by

$$v_{\max} = 0.88\sqrt{\pi G \sigma_0 h}. \tag{15}$$

Combination of Eqs. (6) and (15) results in

$$v_{\max} = 0.88 \langle v_z^2 \rangle_{R=0}^{1/2} \sqrt{\frac{h}{z_0}}, \tag{16}$$

where the maximum rotation is reached at a radius of approximately two scalelengths. Note that the result of Eq. (16) does not depend on the photometry of a galaxy; $v_{\max}$ is just the maximum rotation allowed by the mass content of a disk which is expressed in the velocity dispersion. Whether a disk is faint, bright, red, or blue does not change any calculations or influence any of the subsequent conclusions in this section.

For various values of h/z_0 the relation in Eq. (16) is shown in Fig. 6 together with the observations. Also, the curve for h/z_0 following from a constant $(M/L)_B$ of 2.0 is given. As can be seen, all data lie below this curve, and even all data lie below the lines for realistic h/z_0 values. The argument can be turned around by saying that, to bring the data in agreement with the curves a value of h/z_0 between 10 and 25 is needed, which is certainly unrealistic. What this all means is that the observed disk dispersion only allows a much smaller maximum rotational velocity produced by the disk than what is observed. To make matters quantitative, for the sample of twelve galaxies the maximum attainable disk rotation has been calculated, using the h/z_0 values of Fig. 4a given by the dashed line in Fig. 6. The calculated value is compared with the actually observed maximum rotation and it appears that *the maximum rotation supplied by a disk is on average 63% of the observed maximum rotation, roughly independent of the size of the galaxy*. There is a considerable scatter onto this 63%; a range is found from 45% to 80% but most galaxies are within 10% from the average result. The situation can be illustrated by considering the well studied spiral NGC 3198 (van Albada et al. 1985; Begeman 1987), which has an observed maximum rotation of 157 km s^{-1}. For a dispersion $\langle v_z^2 \rangle_{R=0}^{1/2}$ of 40 ± 7 km s^{-1} and a realistic h/z_0 value of ~ 6 the disk can only contribute 86 ± 15 km s^{-1} to the rotation. A similar reasoning can be applied to other individual galaxies, for instance our Galaxy (van der Kruit 1987b; Schmidt 1985) or NGC 891 (Bottema et al. 1991) reaching the same conclusions.

Combination of photometric and kinematical data allows the construction of mass models using a disk with constant M/L and spherical halo (Carignan & Freeman 1985; van Albada et al. 1985; Bahcall & Casertano 1985; Kent 1986). By most authors a solution is favoured which maximizes the contribution of the disk to the observed

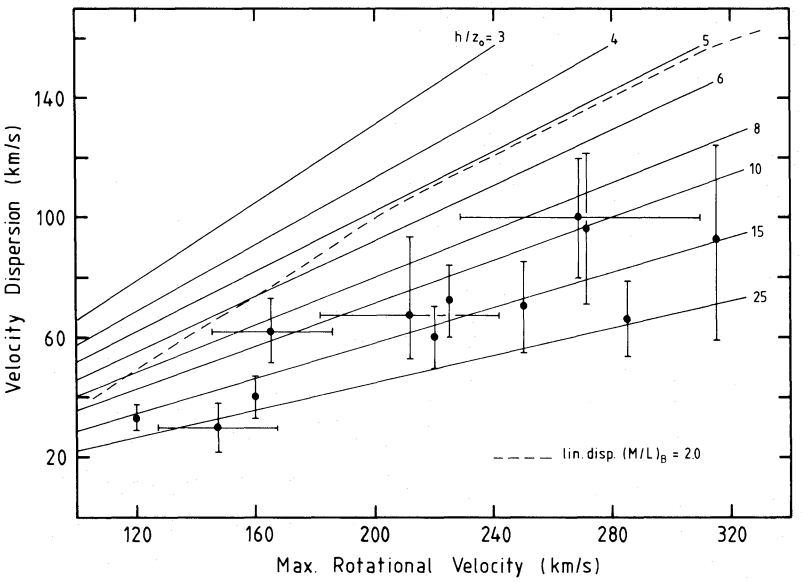

Fig. 6. The maximum rotational velocity that is allowed for a galactic disk with a certain velocity dispersion. Drawn lines are for different values of constant h/z_0, the dashed line for the h/z_0 behaviour as in Fig. 4a. For a realistic thickness of a disk the curves lie above the data. It appears that the disk contributes, on average, only 63% to the observed rotation, essentially independent of the mass of the galaxy

rotation, resulting in the postulation of the so called "maximum disk hypothesis" (van Albada & Sancisi 1986). Several arguments are presented supporting this hypothesis, but none of these constitute any hard evidence. In general a range of solutions is possible going from no disk at all to maximum disk. Still, this range is constrained mainly by stability arguments (Athanassoula et al. 1987) because too small a disk cannot form any spiral structure and a too large disk contribution may be unstable to $m=1$ distortions. Even, for the maximum disk solution the maximum rotation of the disk is on average $\sim 10\%$ lower than the observed maximum rotation in order to prevent the dark halo to have a hollow core. The present study shows that on average a disk supplies 63% of the observed maximum rotation. Onto this 63% there is some scatter of 10% part of which, considering the data, is real, indicating that different galactic disks contribute differently to the rotation. Still, over the observed range of brightness a maximum disk solution, with a disk supplying 90% of the observed maximum rotation is not possible. On the other hand the disk does dominate the rotation at the radii where it reaches its maximum value.

The conclusions presently deduced are important and their solidity has to be assessed. Therefore a discussion will be given to determine the errors (systematic and random) of the calculated maximum rotational contribution of 63% for the average disk. First, the systematic errors that may occur (numbered S1 to S5).

(S1): changing from sech² to sech

As discussed in Sect. 2, a deviation from a locally isothermal disk situation could be actual. This deviation is such that close to the plane the stars are cooler, but the vertical dispersion behaviour cannot be more deviant from isothermal than a resulting density behaviour of a sech(z) nature (van der Kruit 1988). Changing from the isothermal sech²(z) to a sech(z) vertical density profile results in increasing the numerical factor of 0.88 to 0.95 in Eq. (16). This changes the average disk maximum rotation from 63% to 68% of the observed maximum rotation.

(S2): thick disk instead of Freeman disk

Equation (15) is for an infinitely thin Freeman (1970) disk. If a disk has a thickness of $h/z_0 \sim 5$, then the numerical factor 0.88 has to be decreased to 0.84 (Casertano 1983). This means decreasing the disk amount of rotation from 63% to 60%.

(S3): influence of dark halo on velocity dispersions

According to Sect. 9 a dark halo may result in, at least for $R \gtrsim h$, measured dispersions which are somewhat larger than the dispersions of an isolated isothermal disk. After fitting a curve to the data of an individual galaxy, over the extent of the radii of observations, this can effectively result in the numerical factor 0.88 to be too large by at most a few percent.

(S4): other functionality than $\langle v_R^2 \rangle^{1/2} \propto \sqrt{\mu(R)}$

This can only be the case for the galaxies which have observed dispersion values at only a few radial positions. But then, still, the observations remain the same and the calculable surface density over the radial extent of the observations will result in a locally determined ratio of disk mass to total mass. The photometry of the whole disk, which is exponential for an average disk, then provides the amount of rotation the disk can supply resulting in the same 63%.

(S5): bulge influence

The only galaxies of the sample for which the bulge provides a significant contribution to the total rotation at the position where the disk has its maximum velocity are NGC 2815 and NGC 2613. For the latter galaxy matters are uncertain because there is no precise photometry. For NGC 2815 the bulge rotation as given by Kent (1986) has been quadratically subtracted from the total rotation giving a maximum rotation of 220 km s^{-1}. That value is used in the calculations.

Secondly the random errors (R1 and R2).

(R1): uncertainty in h/z_0 *(Fig. 4)*

There is a scatter of a factor 1.4 in h/z_0 related to the 0.4 mag scatter in Freeman's law. This causes a scatter of a factor 1.18 in the calculated maximum disk rotation from the dispersions; resulting in an amount of disk rotation of $63\% \pm \sim 10\%$, which is roughly what is observed.

(R2): departures from exponential disk

This gives maximum rotational velocities which scatter "around" Eq. (15). Because the maximum rotation is a result of an integration over the disk mass distribution, this scatter will be small, within a few percent.

Summarizing the discussion, the possible systematic errors are relatively small and tend to cancel one another. The random errors are significant but in agreement with the observed random deviation from the average value. There is simply no way to increase the average disk rotational level of 63% with a substantial amount to levels of 85% to 90%. Hence, the fact that the calculated maximum disk rotation is systematically and substantially lower than the value of the maximum disk hypothesis is well established.

6. The Tully–Fisher relation for galactic disks

The linear dispersion luminosity relation from Eq. (5) combined with the maximum rotation Eq. (16) and relation

(10) which holds for a pure disk system converted to M_B $(H_0=50)=M_{od}-1.38$ results in

$$M_B(H_0=50)=-0.0668 v_{max}\sqrt{\frac{z_0}{h}}-17.76. \quad (17)$$

This relation between luminosity and maximum rotational velocity is compared with Rubin et al.'s Tully–Fisher picture in Fig. 7. For constant values of h/z_0 curves are given which show that h/z_0 needs to be around 10 in order to make Eq. (17) for disk only systems in agreement with the observations of the (comparable) Sc galaxies.

Equation (17) gives a luminosity directly proportional to the maximum rotational velocity. That, however, is not very realistic. If Freeman's law applies and M/L is the same for all galaxies one arrives at the original explanation for the T–F relation by Aaronson et al. (1979) namely

$$M_B=-10\,^{10}\log(v_{max})+C. \quad (18)$$

The data of Rubin et al. indeed imply a coefficient very close to the desired value of 10. Recollecting the reasoning in Sect. 4 arguing for equal mass-to-light ratios I shall thus assume Eq. (18) to be valid and explore the consequences. In the previous paragraph the relation between dispersion and luminosity was taken to be linear [Eq. (5)]. Instead into Eq. (18) relation (16) will be inserted and the dispersion luminosity relation is derived:

$$\langle v_z^2\rangle^{1/2}=A^{-1}\sqrt{\frac{z_0}{h}}10^{-0.1M_{od}}, \quad (19)$$

with

$$A=0.88\ 10^{-0.1(C+1.38)}, \quad (20)$$

choosing a certain behaviour of z_0/h as a function of M_{od} completes Eq. (19) which can then be compared with the dispersion data in Fig. 2 and a value for A is determined. This again gives the value for C which can be substituted back into Eq. (18) and the "disk only" Tully–Fisher relation is found. Choosing the functionality of z_0/h should, of course, be such that the dispersion luminosity relation reasonably fits the observations. Some further manipulations yield another useful result. Rewriting Eq. (11) without the explicit dispersion relation gives

$$\left(\frac{M}{L}\right)_B\left(\frac{z_0}{h}\right)=1.04\langle v_z^2\rangle 10^{0.2M^B_{od}}, \quad (21)$$

and if Eq. (19) is substituted

$$\left(\frac{M}{L}\right)_B=1.04\ A^{-2}. \quad (22)$$

So as bonus the mass-to-light ratio of the disk is found independent of h/z_0!

Three examples of three different z_0/h behaviours will be discussed as illustrated in Fig. 4a. First, $h/z_0=5$ constant, independent of galaxy luminosity. Substitution into Eq. (19) gives a relation which is compared with the dispersion data in Fig. 8a. As can be expected, the relation does not give a perfect fit, but still is in reasonable

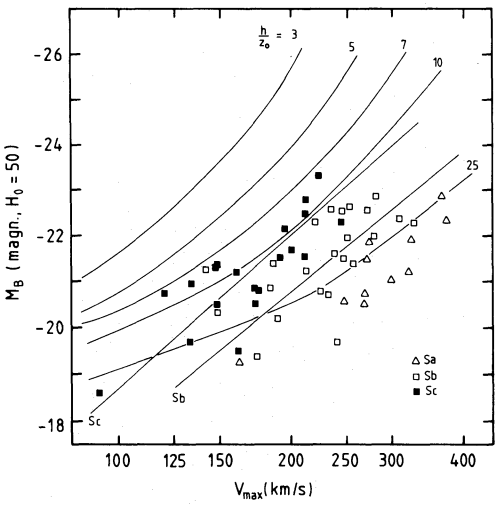

Fig. 7. Predicted galactic disk Tully–Fisher relation for the linear dispersion–luminosity relation of Fig. 2 and constant values of h/z_0, compared with the Rubin et al. (1985) data

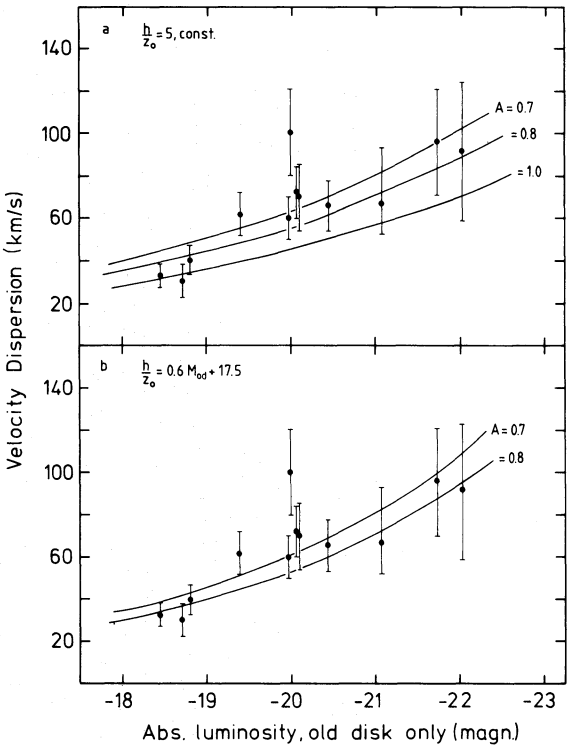

Fig. 8a and b. Fit to the observed dispersion data for a "slope ten" (Eq. 18) Tully–Fisher relation and so implied equal mass-to-light ratios. **a** For h/z_0 equal to five; the data cannot be fitted perfectly, but the fit is reasonable for $A=0.8\pm0.1$. **b** For an h/z_0 functionality indicated by the dash-dot line in Fig. 4a; the best fit is achieved for $A\sim0.75$. The parameter A is defined by Eqs. (18)–(20) and determines the intercept of the T–F relation

agreement with the observations for $A=0.8\pm0.1$. From Eq. (20) then follows $C=-0.97\pm0.5$ and $(M/L)_B=1.75\pm0.4$. In the second example z_0/h is chosen such that the dispersion luminosity relation is linear [Eq. (5)] and $(M/L)_B=2.0$. According to Eq. (11)

$$2.0\left(\frac{z_0}{h}\right)=1.04\{-17M_{\rm od}-279\}^2 10^{0.2M_{\rm od}}, \quad (23)$$

which, when substituted into Eq. (19) gives

$$\langle v_z^2\rangle^{1/2}=A^{-1}0.72\{-17M_{\rm od}-279\}, \quad (24)$$

making a good fit to the observations for, of course, $A=0.72$ and $C=-0.51$. For the last example a linear relation between h/z_0 and luminosity is adopted: $h/z_0=0.6M_{\rm od}+17.5$. Then in Fig. 8b the relation resulting from Eq. (19) is compared with the data showing a good fit with $A=0.75$. This results in $C=-0.69$ and $(M/L)_B=1.85$.

The T–F relation for a disk as given by Eq. (18) with the three different C values which have just been determined is compared with total galaxy data in Fig. 9. Results for the various h/z_0 functionalities are similar; a relation is found which lies above the observations. This implies that a disk with a certain luminosity only provides a part of the observed maximum rotation. In fact, this is the same result as found in the previous section but now it is cast into a Tully–Fisher representation. The additional information that comes out is that the whole picture is consistent. The same M/L for all galaxies which has to give a slope of ten in a luminosity rotation relation can provide a dispersion luminosity relation which fits the data for a certain h/z_0 behaviour for which a constant M/L ratio applies again.

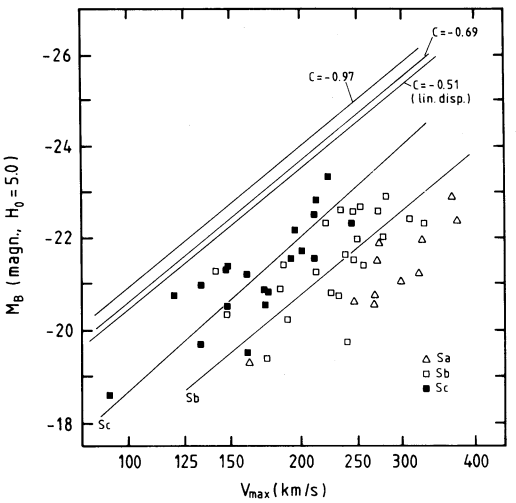

Fig. 9. The galactic disk Tully–Fisher relation for equal mass-to-light ratios. The results for three different h/z_0 functionalities are given compared with the Rubin et al. data. As is obvious, the observed velocity dispersions of galactic disks give a relation lying above the observed T–F relation for comparable Sc systems, which again is a result of the fact that the disk supplies only a part of the observed maximum rotation

The location of the "disk only" T–F relation is also fixed, which gives a proper starting point for a discussion of the observed magnitude–maximum rotation data.

Rubin et al. (1985) find a morphological type segregation (Fig. 9) for their sample. Even in the infrared this segregation does not disappear completely and the same scatter per type remains. Other studies of the T–F relation, which generally use the H I line profiles to get the rotation, do not or not clearly find the segragation (e.g. Aaronson et al. 1982; Aaronson & Mould 1983). The different findings must be explained by sample selection effects and likely by the better determined rotation following from the optical spectral observations. Type segragation in the B band originates mainly from population effects. Going along the Hubble sequence from Sc to Sa, first the disk becomes redder because there is less star formation, and secondly a bulge is added being a pure red old disk population. The result is a change in average (over the whole galaxy) $(M/L)_B$ along the Hubble sequence. In the near infrared these population effects are less apparent but not negligible. The segragation is also caused by secondary effects namely that the additional light of the bulge does not obey $M_B\propto 10^{10}\log(v_{\rm max})$ because the bulge is rounder and more concentrated and also the maximum rotation of the bulge does not appear at the same radius as for the disk. In the present paper calculations are only limited to a one colour disk; a more extended discussion properly incorporating actual colours and bulge/disk ratios is beyond to scope of this article. Of course, a comparison of the results with Sc galaxies is always valid.

A matter which might be explained, at least partly, is the scatter of the observed blue and near IR T–F relation. If the ratio of dark to luminous matter is different for different galaxies, for a disk with certain luminosity the shift to higher velocities because of the halo can create an appreciable scatter in the T–F relation. This effect then mimics the result of a scatter in the total M/L ratio, which is usually inferred to explain the T–F scatter. The present picture is to be favoured because now the mass-to-light ratio is universal (for a constant colour or in the infrared), a fact that arises from an expected similar star formation process for galaxies. Of course, over the whole range of absolute luminosities, on average, the disk to dark halo mass ratio has to be equal or else the slope of ten cannot be explained (van Albada et al. 1985).

7. The Q criterion

Both, the random motions and rotation, which is a reflection of the disk–halo ratio, of a disk can be combined into Toomre's (1964) Q parameter. Presently it will be calculated and in first instance treated as an observable quantity. Later on the results will be compared with theoretical calculations and implications and relevance will be discussed.

Toomre's Q value is given by

$$Q=\frac{\langle v_R^2\rangle^{1/2}\kappa}{3.36G\sigma}, \tag{25}$$

where κ is the epicyclic frequency which can be derived from the rotation curve and σ the projected surface density. For an exponential galactic disk with surface density $\sigma=\sigma_0 e^{-R/h}$ and dispersion $\langle v_R^2\rangle^{1/2}=\langle v_R^2\rangle_{R=0}^{1/2} e^{-R/2h}$ the following rotation curve is adopted (Fall & Efstathiou 1980)

$$v_{\rm rot}=v_{\rm max}\sqrt{\frac{R^2}{R^2+d^2}}. \tag{26}$$

Substitution of the above relation into Eq. (25) gives

$$Q=0.10\left(\frac{\langle v_R^2\rangle_{R=0}^{1/2}}{\rm km\ s^{-1}}\right)\left(\frac{\sigma_0}{M_\odot\ {\rm pc}^{-2}}\right)^{-1}\left(\frac{v_{\rm max}}{\rm km\ s^{-1}}\right)\frac{F(R,h,d)}{\rm kpc^{-1}}, \tag{27}$$

with

$$F(R,h,d)=e^{R/2h}\left(\frac{\sqrt{R^2+2d^2}}{R^2+d^2}\right). \tag{28}$$

Now first this radial part of Eq. (27) will be considered. It is demonstrated by Rubin et al. (1985) that rotation curves of spiral galaxies are qualitatively the same except for a constant factor putting the flat part at a higher level for brighter galaxies. The radius at which the rotation curve turns over, however, is practically equal for all systems. From Rubin et al.'s Fig. 6, when interpreted in terms of Eq. (26), it is deduced that the value of $d\approx 1.4$ kpc ($H_0=75$) independent of the brightness of a galaxy. To eliminate another variable the scalelength h will be expressed in the maximum rotational velocity. There are two ways to accomplish this. First, Table 4 can be used with the Tully–Fisher relation to derive the desired relation for a pure disk. A second, more general, method has been used however which gives a little different scalelengths but the final result is practically insensitive to which method is used. This second method is based on the relatively strict relation between R_{25} and brightness of a galaxy given by Rubin et al. for Sb to Sc galaxies

$$\log(R_{25})=-3.9-0.245M_B\ (H_0=50)\ \text{(in kpc)}, \tag{29}$$

using $R_{25}\sim 3.1\times h$ following from Freeman's law and

$$M_B(H_0=50)=3.0-10.6\ {}^{10}\log(v_{\rm max}), \tag{30}$$

Rubin et al.'s T–F relation for Sb to Sc galaxies one finds

$$\frac{h}{\rm kpc}=4.95\ 10^{-6}\ v_{\rm max}^{2.6}. \tag{31}$$

This relation is tabulated in Table 5 together with the result for a pure disk. The radial part of the Q parameter is calculated and shown in Fig. 10 for different values of $v_{\rm max}$.

Table 5. Scalelength of a galaxy with different max. rotational velocities

$v_{\rm max}$ (km s^{-1})	h disk only (kpc)	h acc. to Eq. (31) (kpc)
100	1.22	0.78
125	1.95	1.40
150	2.87	2.25
200	5.29	4.76
250	8.49	8.50
300	12.49	13.65

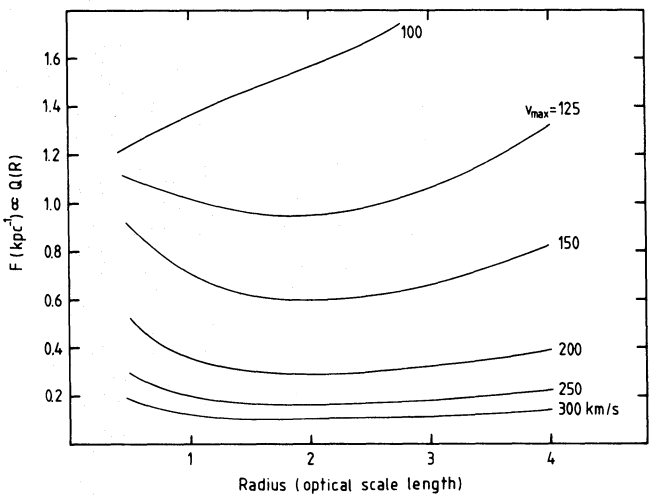

Fig. 10. Radial behaviour of Toomre's Q parameter for an exponentially decreasing velocity dispersion ($\propto e^{-R/2h}$) of a galaxy having different values of maximum rotational velocity. In general Q is rather constant, or, a model with constant Q would also have fitted the dispersion data for individual systems

It is obvious that the dependence is weak: over a large radial extent the value of F [Eq. (28) and hence Q] is rather constant. This conclusion has been reached earlier for more specific cases by Bottema et al. (1987) and by Martinet (1988). Therefore one might consider to replace $F(R,h,d)$ by the average value over the radial extent of a galaxy. This has not been done; instead for F the value at one scalelength has been taken because of the following reason: Velocity dispersions are generally measured between a radius of a half to two scalelengths. At smaller radii the bulge becomes dominant, at larger radii a galaxy is too faint. If instead of an exponentially decreasing dispersion model a dispersion model for an adopted constant Q would have been fitted to the data the parameters of the latter model would have been fixed at a radius of approximately one scalelength.

Quite some assumptions have been used to determine the radial dependence of Q but any reasonable change of these assumptions will not alter the results significantly.

Therefore one can safely fill in the F-value in Eq. (27) and replacing σ_0 with $\mu_0^B(M/L)_B$ where $\mu_0^B = 136\ L_\odot\ \mathrm{pc}^{-2}$, Eq. (27) can be rewritten to

$$\langle v_R^2 \rangle_{R=h}^{1/2} = \frac{816\ Q(M/L)_B}{v_{\max}\ F(v_{\max}, R=h)}. \tag{32}$$

This relation can be explored when projected onto Fig. 2, the relation of dispersion versus maximum rotation. To this aim, first, the same value of $Q = 1.7$ has been adopted (explanation will follow below) for all galaxies which results in the curves depicted in Fig. 11a. The result is quite striking; for a constant value of $(M/L)_B = 2.8$ with a scatter of about 0.5 relation (32) traces the observations nicely. The argument has been turned around by taking $(M/L)_B = 2.0$ as suggested in the previous sections. Relation (32) is now shown in Fig. 11b for $Q = 2$ and 3, again the data are traced excellently for Q between 2 and $2\frac{1}{2}$ over a large range of maximum rotational velocity. Hence an important conclusion can be reached namely that the same M/L ratio for galactic disks implies that the Q value is also equal for all disks, and vice versa. This is a pure observational result, not affected by any theoretical model.

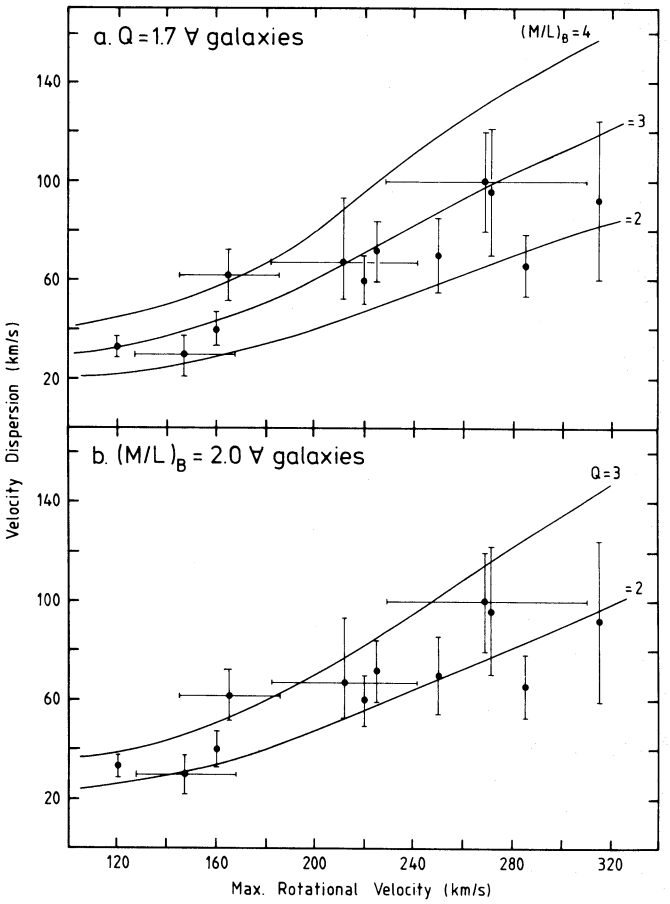

Fig. 11a and b. Implications of a constant Q value for all galaxies superposed on the observed dispersion maximum rotational velocity data. **a** When $Q = 1.7$ the mass-to-light ratio appears to be constant around 2.8 and turning the argument around: **b** When $(M/L)_B = 2.0$, Q is constant between 2.0 and 2.5. The latter is equal to the general global stability criterion found by Athanassoula & Sellwood (1986)

To relate the findings above to theoretical concepts is difficult. Starting from basic theoretical concepts to derive the actually observable stellar velocity dispersions seems impossible (Binney & Lacey 1988). Two other approximations of the matter of disk stability and evolution have been and are being pursued. There are N-body numerical pure stellar studies by a.o. Carlberg & Sellwood (1985), Sellwood & Carlberg (1984), Villumsen (1985), Sellwood & Athanassoula (1986), Athanassoula & Sellwood (1986) and Sellwood & Lin (1989). And the other approximation is a modal study of a one (only stars) or two component (stars + gas) fluid model by a.o. Lin & Bertin (1985), Bertin & Lin (1987), Bertin et al. (1989a, b) and Bertin & Romeo (1988) as an extension to the original Lin & Shu (1964) theory. All studies have common shortcomings like only two dimensions, no separation of old-disk and young population and hence no secular stellar evolution. The N-body simulations have no gas component included and are restricted to a specific mass model but allow non linear processes. On the other hand, the hydrodynamical fluid model does include a description of the gas influence and has more realistic galaxy mass models, but is restricted to [as stated by Sellwood & Lin (1989)] "slowly growing spiral modes for which very specific conditions are required". As will be obvious, there is not a well established description of the stellar dynamics in spiral galaxies. There is a matter on which all studies agree and that is the existence of a so called "self regulation" mechanism (Bertin & Lin 1987). In short what this amounts to is that in a galactic disk there is a cold gas layer from which young "cold" stars are born. These young stars cool the stellar disk, generating spiral instabilities and hence spiral arms, which heat up the disk. But also these arms generate new stars which again cool the disk. In this way a stable situation will establish which shows up as the normal spiral pattern as observed.

The only study where this self regulation is partly simulated is by Sellwood & Carlberg (1984). The result is that the Q value approaches a constant value around 1.7 over the entire stellar disk. This constant level is very appealing since, as has been shown above, the exponentially decreasing velocity dispersion generates a radial Q behaviour which is rather constant with radius. Thus this result of Sellwood & Carlberg is in agreement with the kinematics of real galaxies. Unfortunately they use a rather large halo to disk ratio and likely a smaller ratio would allow the disk to heat up till larger Q values while maintaining the spiral structure, having a more open appearance (Athanassoula & Sellwood 1986). In fact, the final Q value will likely depend only on the parameter halo/disk ratio as long as there is sufficient gas to sustain the self regulation. Consequently, if this ratio is nearly

equal for all galaxies one may expect a universal equilibrium Q_{eq} for all galaxies. What is then the value of this Q_{eq}? Well, Athanassoula & Sellwood show that $Q_{stellar} \gtrsim 2$–2.5 is a sufficient condition to prevent barlike instabilities irrespective of the halo/disk ratio. Therefore one can also expect (for non barred galaxies) the Q_{eq} to range between 2 and $2\frac{1}{2}$. The observations in this paper are of the old stellar population making up nearly all the mass in a disk and being comparable to the stellar dispersions in the numerical simulations. If I therefore take over a universal Q value between 2 and $2\frac{1}{2}$, Fig. 11b shows that the mass-to-light ratio of disk is close to two. This is in excellent agreement with the results of Sect. 4.

8. Re-evaluation of the stellar kinematics of NGC 7184

Spectroscopic observations of the spiral galaxy NGC 7184 are presented by van der Kruit & Freeman (1986). Since the appearance of this paper more sophisticated modelling tools have been developed which will presently be applied to the available data.

NGC 7184 is a regular Sb system (Sandage & Tammann 1981) with a small bulge and/or central bar. It is one of the intrinsically brightest nearby galaxies with a corrected absolute blue luminosity of -23.1 and scalelength of $48'' = 8.4$ kpc, for an adopted distance of 36 Mpc. The galaxy is highly inclined, $i = 75°$ and has a maximum rotational velocity of 266 ± 10 km s^{-1}.

Along the major axis the observed stellar velocity dispersions and asymmetric drift are shown in Figs. 12 and 13 respectively. The difference in radial velocity between the ionized gas and the stars is well established providing four good asymmetric drift values at different radii. The

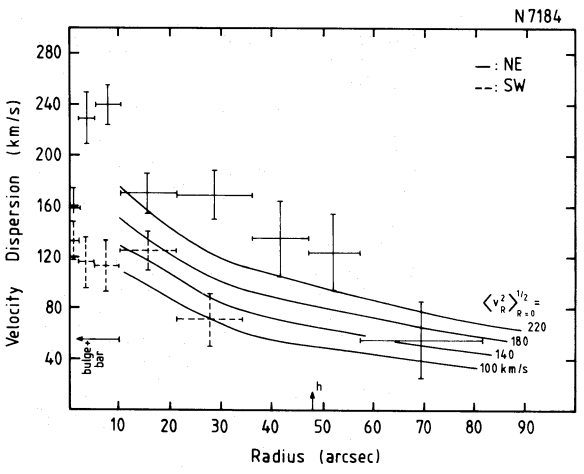

Fig. 12. Observed velocity dispersion along the major axis of the spiral galaxy NGC 7184 by van der Kruit & Freeman (1986). The resulting dispersion an exponential disk would give, for a number of central radial dispersions, is indicated by the lines. The data are irregular and cannot constrain the actual dispersion very well; in this case the asymmetric drift is a better indicator

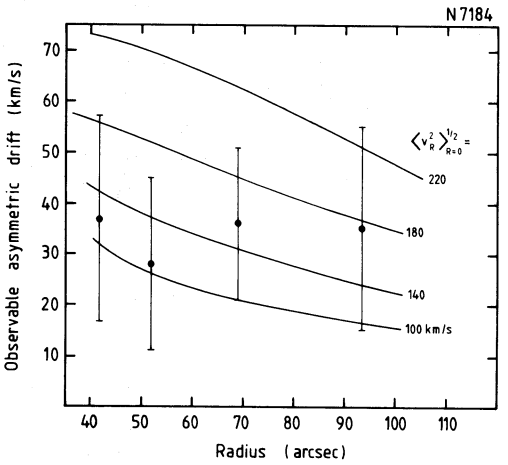

Fig. 13. Observed asymmetric drift values of NGC 7184 (dots) and result of model calculations given by the lines for different central radial dispersions. The best fit is achieved for $\langle v_R^2 \rangle_{R=0}^{1/2} = 140 \pm 40$ km s^{-1}

directly observed velocity dispersion values, however, are not regular. There is a substantial difference between the NE and SW side data in the sense that the dispersions of the NE half of the galaxy are substantially larger. Especially in the bulge/bar inner region the difference is huge which might have to do with the presence of the bar, for it is known that along bars an appreciable stellar streaming will develope (Hohl & Zang 1979). Maybe the central bar activity reaches out to larger radii causing the inconsistent dispersion further out. Also a capture of a satellite galaxy or the existence of a large local instability could be the cause of the observed dispersion behaviour.

A model galaxy has been constructed to explain the data. Essentially the same scheme has been followed as in Bottema (1988, 1989a). For details and equations I refer to those papers and also to van der Kruit & Freeman (1986). The galaxy has been made to consist only of a disk with $\langle v_R^2 \rangle^{1/2} \propto e^{-R/2h}$ and a z_0 scaleheight of 1.5 kpc. From Wray (1988) it is determined that the bulge/bar is confined to within radii of 10″ for which the model obviously cannot apply. The development of a line profile has been simulated by integrating the model. Then model line profiles were compared with the observations. In general integration effects make the observable difference between gas and stellar radial velocities larger than the true asymmetric drift. This effect is dependent on the assumed thickness of the disk; a radially averaged difference of ~ 10 km s^{-1} is found between observable asymmetric drift values for z_0 ranging from 1–2 kpc. The adopted z_0 of 1.5 kpc is for h/z_0 of 5.6, an in every respect reasonable assumption and the error in the calculated observable asymmetric drift because of an uncertainty in the z_0 value will not be larger than 1–2 km s^{-1}. The effect of the thickness uncertainty for the calculated directly observed velocity dispersion is negligible.

The results of the model calculations are given in Figs. 12 and 13 superposed on the observations. The central radial velocity dispersion is made to range from 100 to 220 km s^{-1} and, naturally, both the observable asymmetric drift and dispersion increase when the central dispersion gets larger. From the comparison of model and data it follows that the asymmetric drift observations favour $\langle v_R^2\rangle_{R=0}^{1/2}=140\pm40$ km s^{-1} while for the direct dispersions $\langle v_R^2\rangle_{R=0}^{1/2}=180\pm40$ km s^{-1} gives the best fit. These two values have been averaged, producing a final central R dispersion value of 160 ± 40 km s^{-1} which is 20 km s^{-1} smaller than the value originally favoured by van der Kruit & Freeman. This difference can be fully explained by them making only a preliminary assessment of the appearing integration effects.

9. The effect of a dark halo on the observable velocity dispersion

In Sect. 2 the velocity dispersion as a function of radius has been given for an isolated stellar disk. From recent studies (Begeman 1987, 1989) it follows that it is necessary that a galactic disk is embedded in a dark halo in order to explain the observed rotation curve. Moreover, the previous sections show that even in the inner regions of a galaxy the dark halo gravitational influence may already be appreciable. It thus appears that a galactic disk in general is not that isolated as has been assumed and therefore the effect a dark halo has on the velocity dispersion will be investigated presently.

The basic equations and definitions that describe the z-motion of stars in a disk/halo situation are given by Bahcall (1984). For clarity a summary will be presented. The relevant relations are Poisson's equation

$$\frac{\partial^2\phi}{\partial z^2}=4\pi G(\rho_{\rm Disk}+\rho_{\rm Halo}^{\rm eff}), \tag{33}$$

and the first moment of the Boltzman equation for an isothermal population

$$\langle v_z^2\rangle\frac{\partial\rho(z)}{\partial z}=-\frac{\partial\phi}{\partial z}\rho(z), \tag{34}$$

where ϕ is the total potential and $\rho_{\rm Halo}^{\rm eff}$ the effective halo density, being approximately independent of z and defined by

$$\rho_{\rm Halo}^{\rm eff}=\rho_{\rm Halo}(R)-\rho_{\rm rot}(R)$$
$$=\rho_{\rm Halo}(R)-\frac{1}{4\pi GR}\frac{\partial}{\partial R}V_{\rm c}^2(R), \tag{35}$$

where $V_{\rm c}$ refers to the total (disk + halo) rotational velocity. The following definitions isolate the significant dimensional quantities

$$z_0=\frac{\langle v_z^2\rangle^{1/2}}{\sqrt{2\pi G\rho_{\rm D}(0)}}, \tag{36}$$

$$x=\frac{z}{z_0}, \tag{37}$$

$$y(x)=\frac{\rho_{\rm D}(x)}{\rho_{\rm D}(x=0)}, \tag{38}$$

and

$$\varepsilon=\frac{\rho_{\rm H}^{\rm eff}(z=0)}{\rho_{\rm D}(z=0)}, \tag{39}$$

which allow Eqs. (33) and (34) to be rewritten into one second order differential equation for the dimensionless density distribution $y(x)$:

$$y\frac{{\rm d}^2y}{{\rm d}x^2}-\left(\frac{{\rm d}y}{{\rm d}x}\right)^2=-2y^3-2\varepsilon y^2, \tag{40}$$

with the normalization conditions

$$y(0)=\frac{\rho_{\rm D}(z=0)}{\rho_{\rm D}(z=0)}=1\quad\text{(by definition)}, \tag{41}$$

$$\left(\frac{{\rm d}y}{{\rm d}x}\right)_{x=0}=0\quad\text{(because of symmetry)}. \tag{42}$$

The solution of Eq. (40) for $\varepsilon=0$ has been given by Spitzer (1942) and is

$$y_{\varepsilon=0}(x)=\operatorname{sech}^2(x). \tag{43}$$

For $\varepsilon=0.1$ Bahcall presents a numerical solution and for other small values of ε an approximate analytical formula. Since, certainly for the outer regions of disks the value of ε may be appreciable, numerical solutions of Eqs. (40)–(42) have been calculated for $\varepsilon=0.2$, 0.4, 0.6, 0.8, and 1.0 which are shown in Fig. 14. As can be seen, for an increasing halo contribution the z-density distribution becomes narrower and consequently the disk is containing less matter. The solutions given in Fig. 14 are for a fixed z_0 and fixed dispersion with increasing ε. This is not what one is interested in. Instead for a disk being embedded in a halo, the mass content or surface density remains equal and the only way to achieve this is by increasing the velocity dispersion. Irrespective of the value of ε the z-density distribution can be made broader by multiplying the dispersion by a factor, say α^{-1}, where $\alpha^{-1}>1$. Thus

$$\text{disp}^{\rm new}=\alpha^{-1}\text{disp}^{\rm old}, \tag{44}$$

and so

$$x^{\rm new}=\alpha x^{\rm old}, \tag{45}$$

consequently the new surface density $\sigma^{\rm new}$ is

$$\sigma^{\rm new}=\int_{x=-\infty}^{x=\infty}\rho(x^{\rm new})\,{\rm d}x=\int_{-\infty}^{\infty}\rho(\alpha x)\,{\rm d}x=\alpha^{-1}\sigma^{\rm old}. \tag{46}$$

So if the dispersion increases with a factor α^{-1} then the surface density also increases with a factor α^{-1}. The condition for embedding is that the new (dispersion scaled)

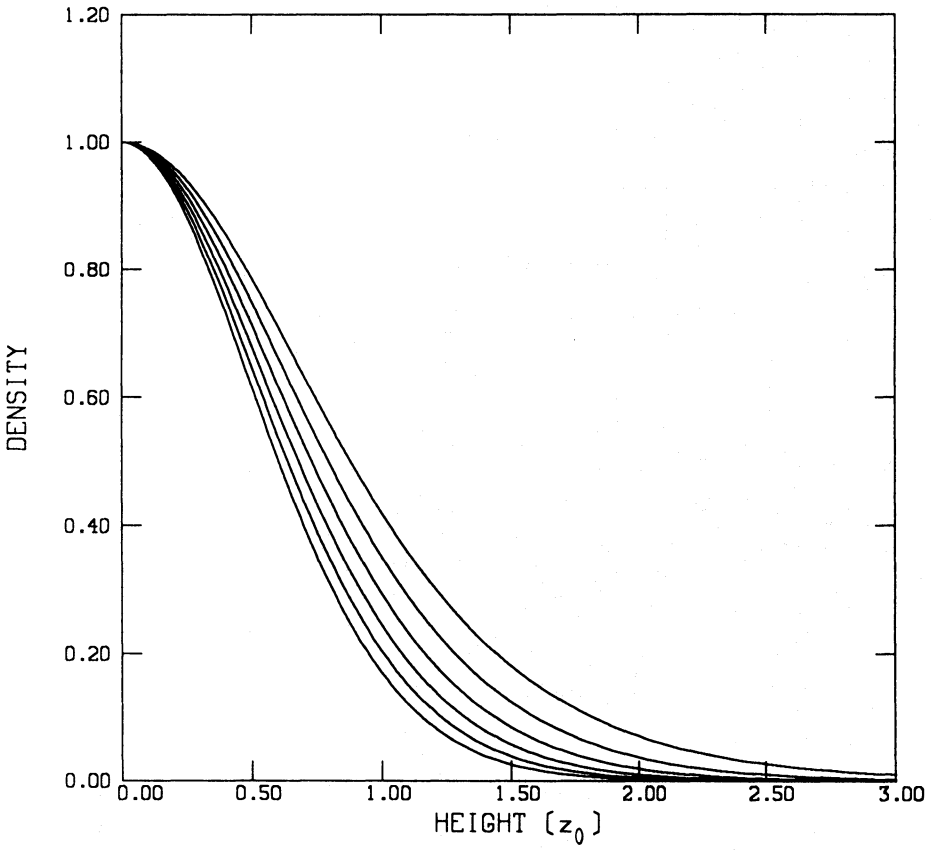

Fig. 14. Dimensionless vertical density distribution of a locally isothermal disk embedded in a dark halo. The sequence from the upper to the lower curve is for an increasing halo mass, expressed in the ε value [Eq. (39)], from $\varepsilon=0$ (nonhalo) to $\varepsilon=1.0$ in steps of 0.2. In this case the velocity dispersion is kept constant which results in solutions with a less massive disk for a larger halo. If instead it is required that the surface density of the disk remains equal, the velocity dispersion has to be scaled for every solution with the inverse of the area under each curve

surface density equals the surface density of the non halo case. The value of the latter amounts to $2\rho_D(x=0)$ calculated by integrating Eq. (43). So, from Eq. (46) follows

$$\alpha_\varepsilon = \frac{\sigma^{\rm old}}{2\rho_D(x=0)} = \int_0^\infty y_\varepsilon(x)\,dx, \qquad (47)$$

such that α_ε is equal to the area under the density distribution curve presented in Fig. 14. Scaling of the dispersion with the factor α_ε^{-1} then ensures that the surface density remains equal to the surface density of the non halo, $\varepsilon=0$, case. Thus, the z-dispersion of a disk in a halo is α_ε^{-1} times as large as the dispersion of an isolated locally isothermal disk. Besides the continuity condition of remaining equal surface density there is another important observational constraint. Any change in ε value as a function of radius must be such that the observed constant disk height as a function of radius (van der Kruit & Searle 1981) remains the same. This disk height is determined by measuring the vertical density (sech^2) profile. For an ε value at a certain position in the disk the calculated z-density, scaled in dispersion with the appropriate amount, thus has to be similar to the isolated disk density distribution. For the solutions depicted in Fig. 14 this has been investigated by scaling the curves in the x-direction with the amount α_ε. It appears that over the whole range of $\varepsilon=0$ to $\varepsilon=1$ the resulting density profiles practically coincide; the difference for the extreme $\varepsilon=1$ case with the isolated disk is at most a few percent. Consequently it can be concluded that embedding in a halo does not change significantly the vertical density profile and any observed radial behaviour of the scaleheight remains the same irrespective of the radial change of ε. Thus curves of Fig. 14 have been integrated and the resulting percentual increase of dispersion as a function of ε is given in Fig. 15. For a very modest halo contribution of $\varepsilon\sim0.1$ a 6% increase is found, for an appreciable halo giving $\varepsilon\sim1.0$ the increase is 52%.

The value of ε can become smaller than zero when $\rho_H^{\rm eff}$ is negative. Still Eqs. (40)–(42) give a solution, but for $\varepsilon\lesssim -0.15$ the density profile is not integratable any more which implies that for a disk the z-dispersion needs to go to zero. Situations of negative ε can occur at small radii with a steeply increasing rotation curve, or only near the central parts of galaxies. At those places the situation differs from that of the rest of the galaxy. First there is generally a bulge which prohibits observing the disk dispersion. The bulge also provides an additional gravitational field and is serving as an enhanced dark halo making the value of ε larger again, an effect that will go beyond the bulge/disk intensity transition radius. Secondly near the central parts of a galaxy for the first moment of the Boltzman equation relation (34) cannot be used any more. Equation (34) is an approximation valid for a plane parallel disk. Near the centres of galaxies this is not the case and terms like $\langle v_R v_z\rangle$ become non negligible and have to be included into

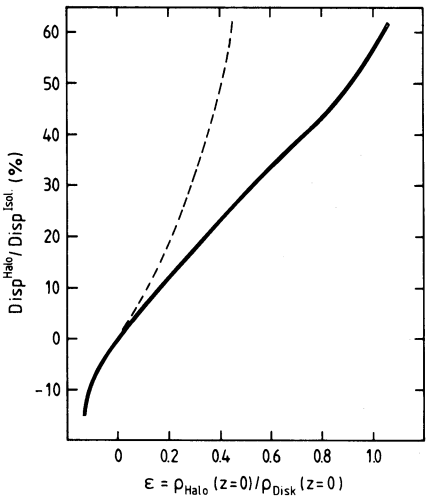

Fig. 15. The vertical velocity dispersion of a disk embedded in a dark halo compared with the dispersion of the same isolated disk. An increasing dark halo contribution is for an increasing ε value. The drawn line gives the exact solution, the dashed line is the result of an approximate analytical solution by Bahcall (1984)

Eq. (34). In order to do this, restrictions have to be imposed on the orientation of the dispersion ellipsoid (Oort 1965) or specific distribution functions and potentials have to be adopted which may give a solution after a complicated calculation (Amendt & Cuddeford 1991). Anyway, the exact consequences are unknown for the position where the bulge is generally dominant. Still, for galaxies with a marginal or no bulge there might be an observable effect. In this respect the strange drop of the dispersion near the centre of NGC 6503 could be a reflection of a negative ε value. However, in general, for a galaxy at positions just outside the bulge the value of ε could be small and negative but then the effect on the observable dispersion is small.

The radial behaviour of ε has been estimated by Bahcall & Casertano (1984) for the Milky Way and three edge-on galaxies. They find values ranging from 0.05 near the inner parts to typically 0.3 near the edge of the disk, implying an additional dispersion over that expected for an isolated disk of about 18% in the outer parts. Obviously, for the systems studied by Bahcall & Casertano both, the photometry and rotation curve are not that well determined. Therefore $\varepsilon(R)$ will be calculated in the case of NGC 3198 for which the mass model is described by van Albada et al. (1985). I have copied their disk and dark halo description and adopted an h/z_0 of 6.8. Two cases are investigated, the maximum disk solution and a solution with a disk mass 0.3 times the maximum disk mass. The latter has a maximum disk rotational velocity of 75 km s^{-1}, certainly constituting a lower limit to the range of possible maximum disk velocities. Logically for a more massive disk the halo belonging to it will be less massive and the resulting ε values smaller. Densities in the plane of the disk (ρ_D), halo (ρ_H) and pseudo rotational density ρ_{rot} have been calculated and the result is given in Fig. 16a. For the maximum disk case the disk is dominant over the halo everywhere. Even for $v_{max} = 75$ km s^{-1}, the disk density contribution is somewhat larger than that of the dark halo. What is striking is that the pseudo rotational contribution is non negligible. In the central parts for the $v_{max} = 75$ case it even completely balances the halo density causing the ε value to stay small near the centre. Figure 16b shows the resulting ε for the two cases and Fig. 16c gives the increase of the dispersion with respect to the dispersion of an isolated disk. Over the radial extent where measurements are available, roughly between a half and two scalelengths, the dispersion becomes larger by at most 20% when the disk is relatively light. Within one scalelength ε becomes negative which will probably not influence the dispersion significantly as discussed above. Finally in Fig. 16d the observed data with the exponentially decreasing dispersion model (Bottema 1988) is compared with the curve a disk would give if it had a maximum rotation of 75 km s^{-1}. This curve is obtained simply by multiplying the exponential model curve with the numbers of Fig. 16c, thus assuming a constant ratio of $\langle v_\Theta^2 \rangle^{1/2} / \langle v_z^2 \rangle^{1/2}$ everywhere. As can be seen, on the basis of the present observations no distinction can be made between an isolated and a "75 km s^{-1}" disk; the difference between the curves for these two extreme cases is only marginal. Whatever the disk contribution is for NGC 3198 the radial dispersion functionality must range between the curves and the assumption of $\langle v_R^2 \rangle^{1/2} \propto e^{-R/2h}$ will always be a good approximation. NGC 3198 is only one example, but for other galaxies one expects the same range of disk/dark halo ratios and roughly the same mass densities. Hence the NGC 3198 results will apply in general. It can be concluded that whether a galaxy consists of an isolated disk, maximum disk or half maximum rotation disk, the dispersions are not significantly different over the region between a half and two scalelengths where this dispersion can actually be observed.

10. General discussion and suggestions for future research

Most of the discussion is presented in the separate sections, therefore only a few additional items will be discussed here; generally in connection with matters that could be further investigated. Until now only of a number of galactic disks the dispersion has been measured. Naturally this sample has to be extended such that the dispersion–luminosity and dispersion–maximum rotation relation can be better determined. More data also allow a better assessment of the ratio between radial and vertical velocity dispersion for external galaxies; now it can only be concluded that a factor of 0.6 is not in contradiction with the observations. Unfortunately, obtaining more dispersion data is easier said than done. Presently it takes one to two nights on a large telescope to observe only one galaxy and data reduction procedures are tedious. A more thorough study

therefore requires lots of telescope time or one has to wait for larger telescopes and/or more efficient high resolution spectrographs.

The larger galaxies seem to have an irregular dispersion behaviour. To investigate this phenomenon a detailed study of an intrinsically bright spiral should be made. Preferably several slit orientations should be observed to determine an as detailed as possible stellar velocity and stellar velocity dispersions field. When the sizes of the irregular areas are determined theories can be developed to explain this phenomenon. For instance, is the irregular stellar field the result of an infall of satellite galaxies or a remnant stellar streaming from the formation of the galaxy?

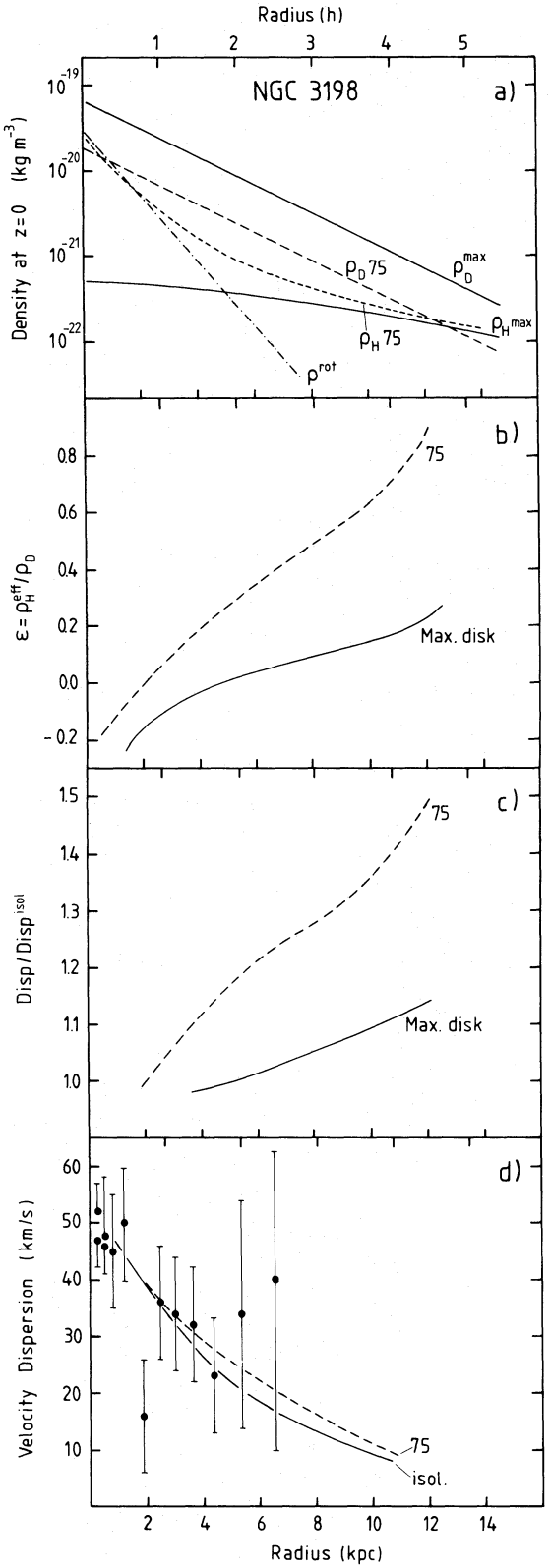

Via Eq. (16) the maximum disk rotation can be calculated when the stellar velocity dispersion is measured. Unfortunately one also has to know the ratio between scalelength and scaleheight (h/z_0). In Sect. 4 a functionality has been calculated, under certain assumptions, favouring an increasing h/z_0 for the fainter disks. But, should there be a relation between h/z_0 and galaxy size anyway? If yes what is the scatter and is it, or can it be observed? There is no direct reason for the existence of this relation because the scalelength is fixed by the composition of the protogalaxy (van der Kruit 1987a; Fall 1983) and the scaleheight is determined by secular heating of the disk by scattering mechanisms. But likely there is an indirect reason; if a disk is forming, a larger disk with a larger rotation may scatter the stars more violently resulting in a larger scaleheight. Therefore some relation between rotation (and hence scalelength) and scaleheight will exist although the exact functionality cannot be predicted easily. Secondary conditions will result in a scatter superposed on the relation. For instance initial star forming efficiency and local surface density may vary for different galaxies. It is however not likely that the present star forming rate, which governs the Hubble type (Sandage 1986), will considerably influence the scaleheight of the existing old disk. Hence no significant correlation will exist between Hubble type and h/z_0 parameter.

It is not only interesting in itself to know the relation between h/z_0 and galaxy size, but it could also support the theories developed in this paper. Unfortunately observations of h/z_0 values are scarce. Only van der Kruit & Searle (1982) present data for eight galaxies of which the value for the small galaxy NGC 5023 is ill determined because of its unknown inclination. An indication that small galaxies are indeed thin comes from Bottinelli et al. (1983) and Heidmann et al. (1972) who show that galaxies of type around

Fig. 16a–d. Calculation of the dark halo influence on the observable dispersions for NGC 3198. Considered are the maximum disk case and a case with maximum rotation of 75 km s^{-1} (indicated by 75). **a** Densities in the plane of the galaxy of the disk (ρ_D) and halo (ρ_H) and pseudo rotational density (ρ_{rot}) for the van Albada et al. (1985) mass models. **b** Resulting ε values. **c** Resulting dispersions compared with the dispersion an isolated disk would have. **d** Comparison with the observed velocity dispersions. It shows that the difference between isolated disk and $v_{max} = 75$ km s^{-1} case is only marginal

Sd, which are generally not massive, have intrinsically the largest flattening. Such small and flat galaxies are usually called "super thin", for which IC 2233 (de Vaucouleurs 1974) and its Southern hemisphere counterpart IC 5249 (Carignan 1983) serve as an example. Because of the very limited amount of measured intrinsic flattening parameters, it is desirable that a project should be started to observe and analyse a larger sample of nearly edge-on galaxies of various sizes and to establish the functionality between h/z_0 and for instance maximum rotation.

The vertical mass density profile near the galactic plane is not known precisely. This causes a fundamental uncertainty in the calculations of the disk surface density from the observed dispersions and hence an uncertainty in the derived maximum rotation a disk can supply. Therefore it is desirable to observe, with sufficient resolution, edge-on galaxies in the optical and near infrared. Such observations together with a proper modelling maybe can achieve an unravelling of a disk in the different populations and dust layer.

An important way to pinpoint down the mass-to-light ratio is by comparing observed velocity dispersions with results of numerical experiments. As discussed in Sect. 7, present numerical investigations suffer from serious shortcomings. Although I am forcing an open door now; numerical experiments should be extended to three dimensions, comprising more realistic galaxy models and including a proper description of the cooling mechanism.

Acknowledgements. The author thanks Piet van der Kruit for helpful discussions and for critically reading the original manuscript.

References

Aaronson M., Mould J.R., 1983, ApJ 265, 1
Aaronson M., Huchra J.P., Mould J.R., 1979, ApJ 229, 1
Aaronson M., Huchra J.P., Mould J.R., Schechter P., Tully R.B., 1982, ApJ 258, 64
Albada T.S. van, Sancisi R., 1986, Philos. Trans. R. Soc. London, Ser. A 320, 447
Albada T.S. van, Bahcall J.N., Begeman K., Sancisi R., 1985, ApJ 295, 305
Amendt P., Cuddeford P., 1991, ApJ 368, 79
Aoki T.E., Hiromoto N., Takami H., Okamura S., 1991, Publ. Astron. Soc. Japan 43, 755
Athanassoula E., Sellwood J.A., 1986, MNRAS 221, 213
Athanassoula E., Bosma A., Papaioannou S., 1987, A&A 179, 23
Bahcall J.N., 1984, ApJ 276, 156
Bahcall J.N., Casertano S., 1984, ApJ 284, L35
Bahcall J.N., Casertano S., 1985, ApJ 293, L7
Begeman K., 1987, Ph.D. Thesis, Groningen State University
Begeman K., 1989, A&A 223, 47
Bertin G., Lin C.C., 1987, in: Palous J. (ed.) Evolution of Galaxies; Pub. Astr. Inst. Czechoslovakian Acad. Sci. 69, 255
Bertin G., Romeo A.B., 1988, A&A 195, 105
Bertin G., Lin C.C., Lowe S.A., Thurstans R.P., 1989a, ApJ 338, 78
Bertin G., Lin C.C., Lowe S.A., Thurstans R.P., 1989b, ApJ 338, 104
Binney J., Lacey C., 1988, MNRAS 230, 597
Bottema R., 1988, A&A 197, 105
Bottema R., 1989a, A&A 221, 236
Bottema R., 1989b, A&A 225, 358
Bottema R., 1990, A&A 233, 372
Bottema R., 1992, A&A 257, 69
Bottema R., Kruit P.C. van der, Freeman K.C., 1987, A&A 178, 77
Bottema R., Kruit P.C. van der, Valentijn E.A., 1991, A&A 247, 357
Bottinelli L., Gouguenheim L., Paturel G., Vaucouleurs G. de, 1983, A&A 118, 4
Carignan C., 1983, Ph.D. Thesis, Australian National University
Carignan C., Freeman K.C., 1985, ApJ 294, 494
Carlberg R.G., Sellwood J.A., 1985, ApJ 292, 79
Casertano S., 1983, MNRAS 203, 735
Disney M.J., Phillipps S., 1985, MNRAS 216, 53
Efstathiou G., Lake G., Negroponte J., 1982, MNRAS 199, 1069
Fall S.M., 1983, in: Athanassoula E. (ed.) IAU Symp. 100, Internal Kinematics and Dynamics of Galaxies. Reidel, Dordrecht, p. 391
Fall S.M., Efstathiou G., 1980, MNRAS 193, 189
Freeman K.C., 1970, ApJ 160, 811
Hohl F., Zang T.A., 1979, AJ 84, 585
Jarvis B.J., Dubath P., Martinet L., Bacon R., 1988, A&AS 74, 513
Heidmann J., Heidmann N., Vaucouleurs G. de, 1972, Mem. R. Astron. Soc. 75, 85
Kent S.M., 1986, AJ 91, 1301
Kent S.M., 1987, AJ 93, 816
Kormendy J., 1983, ApJ 275, 529
Kormendy J., 1984, ApJ 286, 116
Kruit P.C. van der, 1986, A&A 157, 230
Kruit P.C. van der, 1987a, A&A 173, 59
Kruit P.C. van der, 1987b, in: Gilmore G., Carswell B. (eds.) The Galaxy. Reidel, Dordrecht, p. 27
Kruit P.C. van der, 1988, A&A 192, 117
Kruit P.C. van der, Freeman K.C., 1984, ApJ 278, 81
Kruit P.C. van der, Freeman K.C., 1986, ApJ 303, 556
Kruit P.C. van der, Searle L., 1981a, A&A 95, 105
Kruit P.C. van der, Searle L., 1981b, A&A 95, 116
Kruit P.C. van der, Searle L., 1982, A&A 110, 61
Kylafis N.D., Bahcall J.N., 1987, ApJ 317, 637
Larson R.B., Tinsley B.M., 1978, ApJ 219, 46
Lewis J.R., Freeman K.C., 1989, AJ 97, 139
Lin C.C., Bertin G., 1985, in: van Woerden H., Allen R.J., Burton W.B. (eds.) Proc. IAU Symp. 106. The Milky Way Galaxy, Reidel, Dordrecht, p. 513
Lin C.C., Shu F.H., 1964, ApJ 140, 646
Martinet L., 1988, A&A 206, 253
Oort J.H., 1965, in: Blaauw A., Schmidt M. (eds.) Galactic Structure. University of Chicago Press, Chicago, p. 455
Ostriker J.P., Peebles P.J.E., 1973, ApJ 186, 467
Rubin V.C., Burstein D., Kent Ford W., Thonnard N., 1985, ApJ 289, 81
Sandage A., 1986, A&A 161, 89
Sandage A., Tammann G.A., 1981, A Revised Shapley–Ames Catalog of Bright Galaxies. Carnegie Institute of Washington

Schmidt M., 1985, in: van Woerden H., Burton W.B., Allen R.J. (eds.) Proc. IAU Symp. 106, The Milky Way Galaxy. Reidel, Dordrecht, p. 75
Sellwood J.A., Athanassoula E., 1986, MNRAS 221, 195
Sellwood J.A., Carlberg R.G., 1984, ApJ 282, 61
Sellwood J.A., Lin D.N.C., 1989, MNRAS 240, 991
Spitzer L., 1942, ApJ 95, 239
Spitzer L., Schwarzschild M., 1951, ApJ 114, 385
Thuan T.X., Gunn J.E., 1976, PASP 88, 543
Toomre A., 1964, ApJ 139, 1217
Vaucouleurs G. de, 1974, in: Shakeshaft J.R. (ed.) Proc. IAU Symp. 58, The formation and Dynamics of Galaxies. Reidel, Dordrecht, p. 14
Villumsen J.V., 1985, ApJ 290, 75
Wainscoat R.J., Freeman, K.C., Hyland A.R., 1989, ApJ 337, 163
Whitmore B.C., Mc Elroy D.B., Tonry J.L., 1985, ApJ Suppl 59, 1
Wray J.D., 1988, The Color Atlas of Galaxies. Cambridge University Press, Cambridge